Talaromyces marneffei Mp1 protein, a novel virulence factor, carries two arachidonic acid-binding domains to suppress inflammatory responses in hosts

Wai-Hei Lam[1]†, Kong-Hung Sze[2-5]†, Yihong Ke[2-5]†, Man-Kit Tse[2-5]†, Hongmin Zhang[1,6,7], Patrick C.Y. Woo[2-5], Susanna K.P. Lau[2-5], Candy C.Y. Lau[2-5], Simin Xu[2-5], Pok-Man Lai[2-5], Ting Zhou[2-5], Svetlana V. Antonyuk[8], Richard Y.T. Kao[2-5], Kwok-Yung Yuen[2-5]* and Quan Hao[1,6]*

[1] School of Biomedical Sciences,

[2] State Key Laboratory of Emerging Infectious Diseases,

[3] Department of Microbiology,

[4] Research Centre of Infection and Immunity,

[5]Carol Yu Centre for Infection, The University of Hong Kong, Hong Kong SAR, China.

[6] Shenzhen Institute of Innovation and Research, The University of Hong Kong, Shenzhen 518000, China.

[7] Department of Biology and Shenzhen Key Laboratory of Cell Microenvironment,Southern University of Science and Technology, Shenzhen 518055, China.

[8] Molecular Biophysics Group, University of Liverpool, Liverpool L69 7ZB, U.K.

† Wai-Hei Lam, Kong-Hung Sze, Yihong Ke, and Man-Kit Tse contributed equally to this work.

*Correspondence should be addressed to Q.H. (qhao@hku.hk) or K-Y.Y. (kyyuen@hku.hk).

Running title: *T. marneffei* Mp1 protein has two arachidonic acid-binding domains.

Keywords: virulence factor; X-ray crystallography; lipid-protein interaction; NMR; arachidonic acid (AA).

Abstract

Talaromyces marneffei (*T. marneffei*) infection causes talaromycosis (previously known as penicilliosis), the second most-deadly opportunistic systematic mycosis in immuno-compromised patients. Different virulence mechanisms in *T. marneffei* had been proposed and investigated. In the sera of patients with talaromycosis, Mp1 protein (Mp1p), a secretory galactomannoprotein antigen encoding two tandem ligand-binding domains (Mp1p-LBD1 and Mp1p-LBD2), was found to be abundant. Mp1p-LBD2 was reported to possess a hydrophobic cavity to bind co-purified palmitic acid (PLM). It was hypothesized that capturing of lipids from human hosts by expressing large quantity of Mp1p may be a possible virulence mechanism of *T. marneffei*. It was shown that expression of Mp1p enhanced the intracellular survival of *T. marneffei* by suppressing pro-inflammatory responses. Mechanistic study of Mp1p-LBD2 suggested that arachidonic acid (AA), precursor of paracrine signaling molecules for regulations of inflammatory responses, is the major physiological target of Mp1p-LBD2. In this study, we use crystallographic and biochemical techniques to further demonstrate that Mp1p-LBD1, the previously unsolved first lipid binding domain of Mp1p, is also a strong AA-binding domain in Mp1p. These studies on Mp1p-LBD1 support that the highly-expressed Mp1p is an effective AA-capturing protein. Each Mp1p can bind up to 4 AA molecules. The crystal structure of Mp1p-LBD1-LBD2 has also been solved, showing that both LBDs are likely to function independently with a flexible linker in between. *T. marneffei* and potentially other pathogens highly expressing and secreting proteins similar to Mp1p can severely disturb hosts' signaling cascades during pro-inflammatory responses, by reducing the availabilities of important paracrine signaling molecules.

Introduction

Since the first report in 1956, *Talaromyces marneffei* (*T. marneffei*, previously known as *Penicillium marneffei*) is to-date the only known pathogenic species in Talaromyces genus. Along with the AIDS outbreak in late 1980's, talaromycosis caused *by T. marneffei* was the second most-deadly opportunistic systemic mycoses, especially in Southeast Asia region including Northern Thailand, Vietnam, Southern China, Hong Kong and Taiwan (1-4). Healthy hosts can also be carriers of *T. marneffei* but the symptoms of talaromycosis develop only when the immune systems of the hosts are compromised or depressed, for example, in AIDS patients. The first proposed and characterized virulence mechanism of this pathogenic fungus is thermal dimorphism, being able to transit from mycelium form (25°C) to yeast form when its environment reaches host's body temperature (37°C) (5, 6).

In the sera of talaromycosis-positive patients, a galactomannoprotein antigen MP1 protein (Mp1p) was highly expressed and secreted by the infecting fungus (7). ELISA-based kit targeting Mp1p was later developed as a diagnostic test (8). However, it remained unknown why large quantity of Mp1p was produced at the expense of limited resources for *T. marneffei* residing in human hosts.

Mp1p is a 455-residue protein with two tandem domains termed lipid binding domain-1 and 2 (Mp1p-LBD1 and Mp1p-LBD2, residues 28-180 and residues 188-340, respectively), followed by a C-terminal Ser/Thr-rich flexible region which is thought to be the region of O-glycosylations, and a glycophosphatidylinositol-anchor region at the very C-terminus. These two domains share 53% sequence identity and 75% sequence similarity. The crystal structure of domain-swapped (open conformation) Mp1p-LBD2 complexed with a co-purified palmitic acid (PLM) (16:0), a saturated fatty acid for high-energy storage and other cellular processes, was reported (PDB 3L1N), first revealing Mp1p-LBD2 is a fatty-acid binding domain. Mp1p-LBD1 was also described as being unstable in full-length Mp1p and thus only the structure of Mp1p-LBD2 was reported(9).

Later studies on the infectious and survival behaviors of *T. marneffei* suggested that Mp1p is indeed a virulence factor *in vivo*. Life span of mice model challenged by *Mp1*-knockout strain of *T. marneffei* survived up to 60 days without the development of talaromycosis symptoms, while same challenge with wild-type strain could kill the mice within 21 days (10). Subsequent pull-down and lipidomic studies on infected macrophages cell line J774 by *T. marneffei* showed that arachidonic acid (AA), but not PLM, is the dominant fatty acid target of Mp1p *in vivo*. Furthermore, in the same study, it was reported that the productions of both eicosanoids downstream of AA (e.g. prostaglandin E_2) and common markers of pro-inflammatory responses, including tumor necrosis factor-α and interleukin-6, were significantly reduced in murine macrophage cell line J774 after *T. marneffei* infection. Detailed molecular interaction between captured AAs and Mp1p-LBD2 was characterized by various biophysical methods including X-ray crystallography, nuclear magnetic resonance (NMR) titration experiment and isothermal titration calorimetry (ITC). These results together suggested that Mp1p-LBD2, being a strong AA binder, provides a highly-enclosed central hydrophobic cavity (closed conformation) to accommodate up to two AA molecules to suppress inflammation, suggesting a new fungal virulence mechanism (11).

In this study, we focused on the previously uncharacterized LBD1 of Mp1p, Mp1p-LBD1. The crystal structure of Mp1p-LBD1 in complex with co-purified PLM was first solved, providing the first structural proof that Mp1p-LBD1 is also a fatty acid-binding domain. Pull-down assay with Mp1p-LBD1 further suggested that, similar to the previously characterized Mp1p-LBD2, AA is the dominant physiological target of Mp1p-LBD1. Liquid chromatography–mass spectrometry (LC-MS) quantification on isolated endogenous full-length Mp1p from infected murine macrophage cell line showed that the molar ratio of pull-down full-length Mp1p and bound AA is 1 to 4, thus supporting that both LBDs of Mp1p bind AA molecules in a full-length Mp1p *in vivo*. By X-ray crystallography, NMR-titration experiment and ITC assays, the binding mode of AA molecules in enclosed hydrophobic cavity of Mp1p-LBD1 was further characterized. A low-resolution crystal structure of Mp1p-LBD1-LBD2 was solved, suggesting the likely independence between the two LBDs in a full-length Mp1p monomer. The present study thus enhances our understanding on Mp1p, a novel virulence factor of *T. marneffei* playing the central role of a novel virulence mechanism to target and suppress inflammation in hosts.

Results

Mp1p-LBD1 is a fatty acid-binding domain

To begin with our analysis on Mp1p-LBD1, we first purified and crystallized recombinant Mp1p-LBD1 from *E. coli* and solved its crystal structure at 1.80Å resolution. The yield of recombinant protein purified from *E. coli* source is higher than yeast source, making it more suitable for both structural and biophysical studies. This domain forms a complex with co-purified PLM and thus demonstrating that Mp1p-LBD1 also serves as a fatty acid binding domain (Figure. 1A) like Mp1p-LBD2. However, with one molecule per asymmetric unit (ASU), the monomeric protein forms a five-helical bundle structure that resembles Mp1p-LBD2 in complex with AAs (PDB 5CSD), but not the structure of Mp1p-LBD2 in complex with co-purified PLM, which was in an open, domain-swapped form (PDB 3L1N) (Figure.1B). The PLM molecule found in the enclosed central hydrophobic cavity extends from one end to the other, interacting with various hydrophobic amino acid residues along the cavity (Figure. 1D). There is an additional hydrogen bond found between the carboxyl head group of the bound PLM and Gln138 on helix 4. This Gln residue is also involved in hydrogen bond with singly-bound AA in Mp1p-LBD2 (PDB 5CSD), but not PLM. Although both Mp1p-LBD1 and Mp1p-LBD2 can bind co-purified PLM, the orientation preference of the bound PLM is clearly opposite in Mp1p-LBD1 when superimposed to the structure of Mp1p-LBD2-PLM complex (Figure. 2B). This observation of Mp1p-LBD1-PLM complex crystallized in a closed conformation instead of an open conformation as in Mp1p-LBD2-PLM despite the high sequence homology between the two domains, supports the hypothesis that the occupation of ligand near the N-terminus of helix 3 is correlated to whether Mp1p-LBD prefers an open or closed state in the crystal structure, but the underlying mechanism of this different preference remains to be elucidated.

Mp1p-LBD1 can bind up to 2 AA molecules

To elucidate the detailed interaction between Mp1p-LBD1 and its physiological target AA, the complex structure was solved at 2.60Å resolution. Using purified Mp1p-LBD1 after delipidation, excess AA was added for crystallization. The individual monomeric structure of Mp1p-LBD1-AA complex does not differ significantly from the Mp1p-LBD1-PLM complex or the Mp1p-LBD2-AA complex (Figure. 3A and B). There are ten monomers in an asymmetric unit. In two of ten monomers, single AA molecules with characteristic U-shaped conformation can be successfully modeled close to the N-terminal region of helix 3. In another monomer, two AA molecules are successfully modeled, with one of them showing conserved U-shaped conformation and overlapping with the position of the AA in 1-AA bound form, and another AA showing more linear conformation and extending its unsaturated alkyl chain to the other side of the cavity (Figure. 4A). In similar positions in other Mp1p-LBD1 monomers, AA models are left unfitted due to the weaker densities observed.

Superposition of the two AA-bound Mp1p-LBD1 structures to two-AA-bound forms of Mp1p-LBD2 (PDB 5CSD for 1-AA form and 5FB7 for 2-AAs form, respectively) shows that there are slight shifts in the positions of the two AAs in Mp1p-LBD1 due to different hydrogen bond networks involved (Figure. 4B and C). In all solved Mp1p-LBD2 structures, the singly-bound AA forms hydrogen bond with conserved Gln298 while both AAs in the 2-AA bound state form hydrogen bond network with 3 conserved Ser residues, whereas the AAs in both 1-AA and 2-AA bound forms of MP1p-LBD1, make hydrogen bonds with non-conserved Asn105 (Ser265 in Mp1p-LBD2 instead) on helix 3 in Mp1p-LBD1.The longer polar side chain of Asn105 in the central cavity of Mp1p-LBD1 thus provides additional hydrogen bond interaction absent in Mp1p-LBD2 and thus leads to slight shifts of the positions of the AAs in the 2-AA bound forms of Mp1p-LBD1

Singly-bound AA in Mp1p-LBD1 interacts via hydrophobic interactions with Phe36, Leu40, Leu97, Val98, Val101, Val149, Val153 and Leu157 (Left panel, Figure. 3C). The binding of AA_a in the 2-AA bound form also involves same hydrophobic interactions as in the singly-bound AA, except Phe36. In addition, Ser165 also provides hydrogen bond to interact with the carboxylic head group of AA_a (Middle panel, Figure. 3C). AA_b interacts with the following hydrophobic amino acid residues on the other end of the central cavity: Val47, Phe50, Ile72, Val104, Ile108, Leu135, Val168 and Leu172 (Right panel, Figure. 3C). The hydrophobic residues Ile72, Leu97, Val98, Val101, Ile108 and Val149, are involved in both PLM and AA binding in Mp1p-LBD1.

Crystal structure of Mp1p-LBD1-LBD2

We successfully crystallized and solved a double-domain structure of Mp1p from LBD1 to LBD2 as a whole at 4.20Å resolution with 2 molecules per ASU (Figure. 5A). The structure shows that the two Mp1p-LBD1 domains are both in their closed conformation as in

the Mp1p-LBD1-PLM/AA structures reported above, flanking the two Mp1p-LBD2 in their open conformations. This structure is consistent with the individual domain structures of Mp1p-LBD1 and Mp1p-LBD2 complexed with co-purified PLM. The densities corresponding to previously missed linkers between Mp1p-LBD1 and Mp1p-LBD2 in the monomers were observed in molecular replacement solution and built in this model (Figure. 5C and Supplementary Figure. S1A). Moreover, there are minimal contacts observed between Mp1p-LBD1 and Mp1p-LBD2 domains within a Mp1p-LBD1-LBD2 monomer and between two Mp1p-LBD1-LBD2 monomers. These observations suggest that the two Mp1p-LBDs are likely to function independently in the full-length Mp1p. Analytical size exclusion chromatography coupled to static light scattering (SLS) experiments, on the other hand, showed that MP1p-LBD1-LBD2 mainly exists as a monomer (expected size: about 35 kDa) when bound to either co-purified PLM (37 kDa±2.079%) or added AA (34 kDa±2.587%).

Quantification on pull-down endogenous full-length Mp1p show functional redundancies of LBDs

Previously, we have shown that endogenous Mp1p could trap AA by co-immunoprecipitation (co-IP) assays and AA could be identified in the lipid extract of immuno-precipitated products of the *T. marneffei*-infected cell pellet but not from those of the non-infected cell samples(11). In the present study, we have performed quantifications of the pull-down endogenous full-length Mp1p as well as the amount of AA extracted from the Mp1p IP product. The level of Mp1p IP product was found to be 0.864 ± 0.061 pmol per $1x10^6$ J774 cell pellet and the corresponding amount of AA extracted from the Mp1p IP product was 3.10 ± 0.06 pmol. By comparison, the amount of AA extracted was about 4 molar equivalents of that of full length Mp1p, which is consistent with the fact that each of the LBD domains can trap two AA molecules. The present co-IP experiments indicate that in the endogenous full-length Mp1p, each LBD domain has trapped two molecules of AA, suggesting that both domains carried equal functionality in terms of their ability of trapping cellular AA.

Pull down assay and LC-MS study suggest that AA is a physiological binding target of Mp1p-LBD1 of *T. marneffei* Mp1p

Knowing that Mp1p-LBD1 can indeed bind fatty acids leads to speculation that it may also serve to bind other important fatty acids when *T. marneffei* infects host and thus contributes to interrupting hosts' lipid metabolism. We have performed *in vitro* pull-down experiments on the cell lysate of J774 macrophage cells using recombinant His-tagged Mp1p-LBD1 protein in order to identify its potential cellular target. Lipopolysaccharides (LPS) is the standard chemical for inducing the inflammatory responses with up-regulation of cytokines, the lipid mediators and their metabolites. We have used LPS-activated J774 cells in our pull-down experiment to better simulate the lipid profile of infected macrophages. In

order to reveal the dominant higher affinity binding substrates of Mp1p-LBD1, we used progressively lower amount of Mp1p-LBD1 in a series of pull-down experiments. By comparing the results, we could then know the identity of substrates which have higher affinity to Mp1p-LBD1 under the condition of reducing and limited amount of protein. Table 3A lists the identified substrates from the pull-down experiment of Mp1p-LBD1 against the cell lysate of 3×10^6 LPS-activated J774 cells. Three sets of experiments using 1000, 250 and 50 µg of bait Mp1p-LBD1 were performed. When 1000 µg bait protein Mp1p-LBD1 was used, AA, PLM, oleic acid and 4 lysophosphatidylcholines (LPCs) were found in the pull-down profile list. When the amount of bait was reduced 4 times to 250 µg Mp1p-LBD1, AA, PLM, oleic acid LPC1 and LPC2 were found. When we further reduced the bait amount to 50 µg Mp1p-LBD1, all LPCs and PLM were no longer detectable in the pull-down list. These results indicate that Mp1p-LBD1 is capable of binding various lipid substrates but AA is the dominant ligand *in vivo* even though AA was the least abundant in the pool of cellular lipids (Supplemental Table S2 in (11)). The identities of AA, PLM and oleic acid in the pull-down lipid extracts were confirmed by using their pure standards. In negative mode, the peak at m/z 303.2323 and eluted at RT 16.16 min was found to be a significant mass features (MF) in all three pull-down extraction samples (Supplementary Figure 2A). Waters MassLynx Analysis software (Version 4.1, Waters, USA) suggested a molecular formula of $C_{20}H_{32}O_2$ which nicely matched that of AA. Its identity was subsequently confirmed using pure AA standard which showed a well-matched spectrum. The peak at m/z 285 represented a fragment after neutral loss of water from AA while the loss of the polar ester group exhibited the peak at m/z 259. The cleavage of the remaining aliphatic chain contributed to the other fragments observed in the tandem mass spectrometry (MS/MS) spectrum (Supplementary Figure S2A). The identities of the observed LPCs were classified to these lipid classes by their MS/MS fragmentation patterns (Supplementary Figure S2B). The characteristic head group of phosphatidylcholine, m/z=184.1, was applied for detection of phosphatidylcholines and LPCs under positive mode. Fatty acid moieties of identified LPCs were determined using fatty acid scanning (FAS) method as described by Ekroos et al (2003) (12) (Table 3B). According to their characteristic fragmentation peaks, a series of LPCs were putatively identified in the pull-down extraction samples of Mp1p-LBD1 against the cell lysate of J774 macrophages (Table 3A).

NMR-titration and isothermal titration calorimetry (ITC) of LBD1 with AA molecule show two-step binding process

We then verified the AA binding property of Mp1p-LBD1 with NMR and ITC. Figure 7 shows the overlaid 2D ^{1}H-^{15}N HSQC NMR spectra of delipidated ^{15}N-labeled Mp1p-LBD1 (blue-colored cross-peaks) and delipidated ^{15}N-labeled Mp1p-LBD1 after the addition of 3.0 molar equivalent of AA (red-colored cross-peaks). Large and specific changes of amide cross peaks upon the addition of AA indicated that Mp1p-LBD1 could bind to AA and the binding was site-specific. We also carried out isothermal titration calorimetry (ITC) to characterize the binding of AA to Mp1p-LBD1. Figure 8 shows the ITC raw heats of binding and isotherms of AA titrated into wild-type Mp1p-LBD1. The isotherm for titration

of AA into wild-type Mp1p-LBD1 shows a two-step curve and is best fitted with a two-state model similar to that previously observed in Mp1p-LBD2. Fitting of the ITC isotherm with two-site model gives the first binding site a high affinity K_d of 24 nM while the second binding site has a moderate affinity K_d of 2.3 μM. Compared with Mp1p-LBD2 having 13 nM and 2.3 μM for the first and second AA binding K_d's (11), respectively, Mp1p-LBD1's first AA binding K_d is lower but its second AA binding K_d is similar. Since singly-bound AA in Mp1p-LBD1 reported here occupies the same position as the first binding site in Mp1p-LBD2 previously solved (Figure. 4B), we further suggest that the site for the U-shaped AA binding is the high affinity site of Mp1p-LBD1 while the adjacent site for the second linear AA.

Discussion

Talaromycosis caused by *Talaromyces marneffei* is currently the second most deadly opportunistic infection in Southeast Asia, being found mainly in AIDS patients and patients after receiving organ transplantations. One of the key virulence mechanisms known that makes *T. marneffei* exceptionally pathogenic is its thermal dimorphism to transform to yeast form when in hosts(5, 6). It was later reported that expression of Mp1p also plays an important role to suppress hosts' pro-inflammatory responses because its Mp1p-LBD2 can capture released AA during the onset of pro-inflammatory responses to reduce the production of downstream eicosanoids(11). In this study, we have further investigated the previously uncharacterized Mp1p-LBD1 of *T. marneffei* Mp1p, and revealed that it structurally resembles Mp1p-LBD2 in terms of folding and strong two AAs binding property. Each Mp1p thus has two AA-binding domains functioning independently *in vivo*. Although it is logical from the structural point of view that Mp1p-LBD1 and Mp1p-LBD2 may function independently, having two LBD domains with similar biological function may render avidity for Mp1p. In particularly, this might be important for inhibiting and efficient trapping of a ligand. Individually, each binding interaction may be readily broken; however, when many binding interactions are present at the same time, transient unbinding of a single site does not allow the molecule to diffuse away, and binding of that weak interaction is likely to be restored. Antibody is a perfect example for avidity because each antibody has at least two antigen-binding sites, therefore antibodies are bivalent to multivalent. For example, IgM is said to have low affinity but high avidity because it has 10 weak binding sites for antigen as opposed to the 2 stronger binding sites of IgG, IgE and IgD with higher single binding affinities (13)

Despite both Mp1p-LBD1 and Mp1p-LBD2 were first identified as fatty acid-binding domains by the discovery of singly-bound PLM inside their crystal structures, *in vivo* lipid pull-down experiments suggested that both domains bind to AA most specifically when under actual pathological environment inside the host even though other cellular lipids such as PLM, oleic acid, phosphatidylcholines and LPC are more abundant than AA. Although we cannot rule out the possibility that, other endogenous hydrophobic ligands may also pre-occupy the central cavities of the LBDs (for example, PLM). The observation that AA is the only ligand found in Mp1p secreted by *T. marneffei* in macrophage cell line (11) supports

that both the Mp1p-LBD1 and Mp1p-LBD2 domains will soon be occupied by released AA to displace other occupying lipid molecules, during the early steps of pro-inflammatory responses.

Our structural and biophysical analysis on both Mp1p-LBDs in the full-length Mp1p suggested that they are of equal importance in terms of AA capturing and each of them can accommodate two AA molecules. It remains unclear why duplication of LBD is present in *T. marneffei* Mp1p. So far, there is no experimental data on how the full-length Mp1p function would be disrupted *in vivo* when AA-binding function of either Mp1p-LBD1 or Mp1p-LBD2 is abolished by mutations. We suggest that one possible advantage of having two functionally duplicated and independent Mp1p-LBDs in one single protein is to double Mp1p-LBD production efficiency. Fast production of sufficient amount of LBD in the form of full length Mp1p is critical for the survival of *T. marneffei* to effectively reduce the availability of AA because the onset of pro-inflammatory response happens after detection of invasion. Concentration of pro-inflammatory eicosanoids in response to *T. marneffei* infection might reach a threshold to trigger innate immune responses and eliminate *T. marneffei* before sufficient amount of LBD is being secreted and accumulated if the rate of LBD production is slow.

Our low-resolution crystal structure of Mp1p-LBD1-LBD2 first demonstrates that the two Mp1p-LBDs are very likely to function independently since the contact between the two LBD domains is minimal. Moreover, a flexible linker was observed connecting these two domains in a monomer. As expected, two Mp1p-LBD1 domains in this Mp1p-LBD1-LBD2 dimeric crystal structure remain as closed five-helical bundle exactly the same as single domain structure complexed with PLM or AA reported in this study. The Mp1p-LBD2 domains adopt a domain-swapped open conformation exactly the same as the Mp1p-LBD2 structure in complex with PLM (9) (PDB 3L1N). Despite parallel SLS measurement showed that Mp1p-LBD1-LBD2 remains monomeric in solution regardless of bound ligands, this structure disfavors the explanation that the unusual domain-swapped open conformation of Mp1p-LBD2 is due to crystallization because the two structures, Mp1p-LBD2-PLM (PDB 3L1N) and Mp1p-LBD1-LBD2 both reported here, were crystallized in different conditions and space groups, hence different chemical environments for the ASU. Taken together, these observations suggest a model that Mp1p-LBD2 in full-length Mp1p still adopts an open conformation when not bound to AA in solution. Once bound to the released AA from host's pro-inflammatory responses, Mp1p-LBD2 undergoes conformational changes to adopt a closed conformation. Mp1p-LBD1 possibly goes through a different mechanism from Mp1p-LBD2 for AA to enter the central cavity as the closed conformation is the only conformation observed so far.

We have performed ELISA measurements to estimate the level of expression of Mp1p in infected J774 cell samples. At 48 hours post-infection, the levels of free Mp1p were found to be 0.864 ± 0.061 pmol in cell pellet, and 0.116 ± 0.003 pmol in culture supernatant per $1x10^6$ J774 cells, respectively (Supplemental Table S1 in (11)). The free AA concentration varied from cell types and conditions, e.g. 100 µM (inflamed skin tissue), 13 µM (uninvolved skin) (14), 15 µM (resting islets of Langerhans) (15), 0.5-1 µM (resting

leukocytes) (16), (17). Our quantitative MS measurements gave total cellular amount of AA to be 33.0 and 28.2 pmol per pellet of $1x10^6$ J774 cells infected with Mp1p knockout and wild-type T. *marneffei* strains, respectively (Table 2). Therefore, the level of free Mp1p is about 3% that of total cellular AA level. Compared with knockout strain-infected J774 cells, there is 15% reduction of AA level in J774 cells infected by wild-type *T. marneffei*. We believe that this observed level of reduction of AA is reasonable given that each full-length Mp1p can trap multiple molecules of AA. AA is a key proinflammatory signal mediator because it generates the downstream eicosanoid family of mediators. These eicosanoids have potent inflammatory actions, some reaching nanomolar scale, and they can also regulate the production of other mediators including inflammatory cytokines. Since the biosynthesis of eicosanoids depends on the availability of free AA, the base level of free AA in resting cells is under tight control and maintained to be low by locking excess AA into phospholipid pool in esterified form by the action of coenzyme A synthetase (Brash, 2001). In response to infection by microbes, phospholipase A2 is activated to hydrolyze the ester bonds in membrane phospholipids to yield lysophospholipids and AA to initiate the inflammatory response. This is the first line host innate immune defense again microbe infection. In our previous study of Mp1p, we have shown that Mp1p was able to sequester AA with corresponding downstream effects of reducing AA metabolites including PGE2, PGD2, 15-HETE, 11(12)-EET from each of the AA downstream pathways (11). However, no significant changes of AA levels were observed for J774 cells infected with MP1 knockout strain of *T. marneffei* because no Mp1p was expected to be expressed by the MP1 knockout strain (Table 2). Moreover, we also observed a significant increased production of interleukin-6 (IL-6) and tumor necrosis factor-α (TNF-α) for the MP1 knockout strain infected J774 cells (11). Therefore, our present and previous studies on Mp1p have strongly supported that the observed trapping of AA by Mp1p have caused a subtle and significance lowering of cellular AA level with subsequent biological consequences of suppressing downstream AA metabolites and proinflammatory cytokines IL-6 and TNF-α.

Finally, given that the continuous secretion of Mp1p by *T. marneffei* is a demanding task for the pathogen under the limiting environment in the host cell, we believe it is reasonable that the amount of Mp1p secreted will be limited to maintain a near to or slightly lower than base level of cellular AA to evade host innate immune response by dampening the AA downstream pathway of pro-inflammatory signals. It is conceivable that Mp1p is designed to trap more than one AA molecule to increase its trapping efficiency in cells. As far as we know, all known AA binding fatty acid-binding proteins, cyclooxygenases and lipoxygenases interact with one molecule of AA per binding site. Physiologically, this ability to trap more than one AA molecule per Mp1p will improve the efficiency of anti-inflammatory action by Mp1p through encapsulation of AA which will be critical at the initial stage of the *T. marneffei* infection. Furthermore, the plasticity of Mp1p to bind one or more AA molecules with different affinities may reflect the flexibility of this class of AA-binding proteins to sequester AA in response to the abundance of available inflammatory mediators generated by the host.

Following a Domain Enhanced Lookup Time Accelerated BLAST (DELTA-BLAST) search (https://blast.ncbi.nlm.nih.gov/Blast.cgi), many putative Mp1p-LBD1 homologues could be identified in fungal pathogens, such as *Aspergillus flavus and Aspergillus fumigatus* with sequence identity ranging from 23 % to 44 %. The results after filtering the matches for *T. marneffei* are summarized in Supplemental Table S1. We have characterized a number of these putative Mp1p-like homologues of *T. marneffei* for serodiagnosis, including Aflmp1 of *A. flavus* and Afmp1p and Afmp2p of *A. fumigatus (18-24). A. flavus* and *A. fumigatus* are causing aspergilloma and invasive aspergillosis globally and they are the most prominent opportunistic fungal pathogens in immunocompromised host. In our on-going investigations of these Mp1p homologues, we have confirmed that Mp1p homologues Afmp1p, Afmp2p, Afmp3p and Afmp4p are virulence factors of *A. fumigatus(25)* and they can all bind AA in a similar five-helix bundle fold as Mp1p-LBD1 or Mp1p-LBD2 but each only carrying a single LBD rather two LBDs. Full structural and functional characterizations of the binding of AA with Afmp1p, Afmp2p and Afmp4p will be described in a forthcoming manuscript. Here, we showed that these fungi may produce Mp1p or its homologues which could capture AA to stall the inflammatory process. We are in the process of characterizing other Mp1p homologues identified in our studies. This novel function of trapping key pro-inflammatory signaling lipid by "Mp1p-like" virulence factor to evade host innate immunity may be a widely present virulent mechanism in other fungal pathogens. Mp1p thus represents a novel class of fatty acid binding proteins with the function of targeting key proinflammatory signaling lipid to dampen host innate immune response.

Experimental procedures

Construction of expression plasmids for *E. coli* expression system

Full length cDNA of *T. marneffei* Mp1p (strain Mp1) was kindly provided by Prof. KY Yuen's group (Department of Microbiology, HKU). The pair of primers used for Mp1p-LBD1 (a.a. 27 to 182 of full-length Mp1) was CAACAAGGATCCACCAAGGACCAGCGTGATG (Forward) and CTACTCGAGTTAGCTAATGGAGAAGGCTTCG (Reverse). The pair of primers used for Mp1p-LBD1-LBD2 (a.a. 27-342 of full-length Mp1) construct was CAACAAGGATCCACCAAGGACCAGCGTGATG (Forward, same as the forward primer for subcloning of Mp1p-LBD1) and CAACTCGAGTTAAGTGCCGGCGAAG (Reverse). PCR experiments were performed on the provided cDNA to subclone the amplified fragments into an ampicillin-resistant expression vector including N-terminal hexahistidine tag and SUMO tag (His-SUMO) preceding the target fragments with an Ulp1 cleavage site in between, using restriction enzymes BamHI and XhoI (NEB). Following standard protocol of 42°C heat shock transformation and selection with 100μg/mL ampicillin, selected colonies were picked and grown in LB-Broth for plasmids extraction and sequencing (BGI). Correct plasmids were transformed into *E. coli* expression strain BL21(DE3) (Invitrogen) to express the recombinant proteins.

Expression and purification of LBD1 and LBD-LBD2 from BL21(DE3)

4L of transformed BL21(DE3) were agitated at 37°C, 230rpm in LB-Broth with 100µg/mL ampicillin until OD600 was between 0.6 and 0.7. 0.5mM isopropyl-beta-D-thiogalactopyranoside (IPTG) was added for induction at 16°C. After 16 hours of induction, cell pellet was harvested by centrifugation and then was lysed by sonication in lysis buffer (25mM Tris-HCl (pH 7.5), 500mM NaCl and 10mM imidazole). Further centrifugation was performed to obtain the supernatant of soluble total protein. Filtered supernatant was slowly loaded by gravity flow onto 5mL His60 Superflow Ni-IDA resin (Clontech) equilibrated with lysis buffer. After washing with 25mL lysis buffer and same buffer with 50mM imidazole, remained bound protein was eluted with step gradient of 250mM and 500mM imidazole. Fractions containing target SUMO-Mp1p-LBD1 were combined and the His-SUMO tag was released with Ulp1 with simultaneous overnight dialysis against 3L buffer (25mM Tris-HCl (pH 7.5), 50mM NaCl) at 4°C. Cleaved protein was slowly reloaded onto 5mL His60 Superflow Ni-IDA resin equilibrated with buffer (25mM Tris-HCl (pH 7.5), 50mM NaCl). Flow-through containing Mp1p-LBD1 was collected and further purified with 5mL HiTrap™ Q-HP column (GE Healthcare). Target protein was mostly found in the flow-through (Supplementary Figure.S4) and it was concentrated at 4°C with Amicon™ Ultra unit (3kDa cut-off) to 40mg/mL with calculated extinction coefficient 2980$M^{-1}cm^{-1}$.

SUMO-tagged Mp1p-LBD1-LBD2 was overexpressed in the same way as the SUMO-tagged Mp1p-LBD1. The pellet of induced cell was lysed by sonication in lysis buffer (25mM Tris-HCl (pH 8.0), 500mM NaCl and 10mM imidazole). Further centrifugation was performed to remove cell debris. Filtered supernatant was then slowly loaded by gravity flow onto 5mL His60 Superflow Ni-IDA resin (Clontech) equilibrated with lysis buffer. After washing with 25mL lysis buffer and same buffer with 50mM imidazole, remained protein was eluted with step gradient of 250mM and 500mM imidazole The fractions containing the expressed protein with tag was then further purified with 5mL HiTrap™ Q-HP column (GE Healthcare). Protein was eluted in a single peak with linear NaCl gradient. The His-SUMO-tag was removed with added Ulp1 overnight at 4°C with slow agitation for thorough mixing. To obtain the target protein without tag, all cleaved sample was loaded onto 5mL HisTrap™-HP column (GE Healthcare) equilibrated with buffer (25mM Tris-HCl (pH 8.0), 100mM NaCl). Target protein was found in the flow-through with good purity (Supplementary Figure.S4). It was concentrated at 4°C with Amicon™ Ultra unit (10kDa cut-off) to 40mg/mL with calculated extinction coefficient 4470 $M^{-1}cm^{-1}$.

Delipidation on purified protein samples and preparation of AA-bound samples

All recombinant Mp1p constructs from *E. coli* expression systems are found to contain endogenous fatty acids. Delipidation protocol used to remove the endogenous fatty acids was described before on Mp1p-LBD2 (9). Briefly, 5mL of the protein sample was mixed with 4mL of di-isopropyl ether (DIPE) and n-butanol mixture (3:2 (v/v)). The total mixture was agitated gently for 30minutes at room temperature to perform the removal of bound fatty acid and the protein-containing aqueous phase and fatty-acid containing organic

phase were separated by centrifugation (1000g, 10minutes, 4°C). The upper organic phase was removed and fresh organic solvent mixture was added again to repeat the extraction process for at least twice more. 8mL of DIPE was then added to remove the residual n-butanol in aqueous phase. After another centrifugation to separate the two phases, protein was retrieved by penetrating the bottom of centrifuge tube with a needle and 5mL syringe. Dialysis against 1L of buffer (25mM Tris-HCl (pH 7.5), 100mM NaCl) overnight at 4°C was performed on the retrieved protein to further dilute the remaining organic solvent. Delipidated protein concentrations were determined with the calculated extinction coefficients and 6:1 molar excess of freshly prepared 100mM AA dissolved in 100mM NaOH on ice was directly added to the delipidated protein. After incubation for one hour at 4°C, the protein-ligand complexes were concentrated to 40mg/mL and the buffer was intensively exchanged to the buffers of the untreated proteins, with Amicon™ Ultra unit (3kDa cut-off).

Crystallization

The crystals of Mp1p-LBD1 with co-purified PLM (40mg/mL) were grown by mixing 1µL of protein sample with 1µL reservoir solution (0.1M sodium acetate (pH 4.6), 0.2M ammonium sulphate, 20% PEG12000), using hanging-drop vapour diffusion method at 298K. Fully grown and qualified crystals were observed after one week (Supplementary Figure.S4). Cryo-protectant was the same reservoir solution with additional 16% glycerol (v/v). The crystals of Mp1p-LBD1 complexed with AA (40mg/mL) were grown by mixing 1µL of protein sample with 1µL reservoir solution (0.1M sodium acetate (pH 4.6), 0.2M ammonium acetate, 20% PEG4000), using hanging-drop vapour diffusion method at 298K. Fully grown and qualified crystals were observed after 4 days of incubation (Supplementary figure.S4). Cryo-protectant was the same reservoir solution with 16% glycerol (v/v). The needle crystals of Mp1p-LBD1-LBD2 were obtained from crystallization condition 0.1M Tris-HCl pH 8.4, 10mM $NiCl_2$, 1.1 M Li_2SO_4, 5% glycerol (v/v) after two weeks of incubation using hanging drop method at 298K (Supplementary Figure.S4). The cryo-protectant used was the same as mother liquor with 16% glycerol (v/v).

Crystallographic data collection, phasing and models refinement

Diffraction data of Mp1p-LBD1-PLM at resolution 1.80Å were collected at beamline IO2, DIAMOND, Oxford, UK, at 100K. Indexing, integrating and scaling were performed with the XDS package provided on site (26). Data of Mp1p-LBD1-AA at resolution 2.60Å were collected at beamline PROXIMA-I, SOLEIL, Paris, France, at 100K. Indexing, integrating and scaling were performed with HKL2000 package (27). The Mp1p-LBD1-PLM structure was solved with apo-Mp1p-LBD2 structure as a search model (PDB 5CSD) by molecular replacement method (MR) using Phaser in CCP4 package (28). The resultant model of the single solution was then manually mutated to amino acid sequence of Mp1p-LBD1. Refinement was performed with cycles of manual adjustment of model using Coot (29) and Refmac5 (30) included in CCP4 package. Water molecules and PLM molecule were

added and checked manually at last and refined with Refmac5 again to obtain a final model. The dataset of Mp1p-LBD1-AA was solved with the apo-LBD1 structure as a search model for molecular replacement using Phaser in CCP4 package. Refinement was performed with cycles of manual adjustment of model using Coot and Refmac5 also included in CCP4 package. Water molecules and AA molecules were added and checked manually at last and refined with Refmac5 again to obtain the final model. The Mp1p-LBD1-LBD2 dataset at resolution 4.20Å was first solved using molecular replacement with closed apo-Mp1p-LBD1 and apo-Mp1p-LBD2 structures as search models. The density map of single MR solution showed connectivity corresponding to previously unobserved linkers and revealed how the two Mp1p-LBD1 and the two Mp1p-LBD2 are connected. The cross density at the hinge point (Gly259) in Mp1p-LBD2 showed that the both Mp1p-LBD2 domains were in open conformation as in PDB 3L1N (Supplementary Figure.S1). After manual addition of the missing linkers and removal of unseen sidechains due to the relatively low resolution, refinements were performed with cycles of manual adjustment of model using Coot and Refmac5 in CCP4 package including global NCS restraints, jelly-body refinement and Prosmart to generate fragment constraints. The final models are checked with online program MolProbity (31). Data collection and refinement statistics are summarized in Table 1. The Ramachandran plots of the three final structures are shown in supplementary Figure 3. All the graphical presentations of these structures were prepared with graphical software PyMOL (http://www.pymol.org).

Static-light scattering (SLS) to determine molecular weight of Mp1p-LBD1-LBD2 in solution

SLS experiments were performed with the assistance from Dr. Y. Zhao's group (The Hong Kong Polytechnic University, Hong Kong). Purified Mp1p-LBD1-LBD2 samples (with or without AA) were separated with S75 10/300 column (GE Healthcare) already equilibrated with filtered buffer 25mM Tris-HCl (pH 7.5) and 150mM NaCl at 298K. Protein peaks eluted from column were immediately measured with coupled SLS instrument DynaPro Nanostar (Wyatt) using estimated extinction coefficient 4470 $M^{-1}cm^{-1}$. The analysis of protein peaks were performed with the program DYNAMICS provided.

Pull-down experiment on the cell lysate of J774 macrophage cells with Mp1p-LBD1

The J774 murine macrophage cell line was grown in Dulbecco's Modified Eagle's Media (DMEM, Invitrogen) supplemented with 10% heat-inactivated fetal bovine serum (FBS) at 37 °C. Lipopolysaccharide (LPS)-induced inflammatory response was achieved by stimulating the macrophage with 1 g/ml LPS at 37 °C for 24 h. The cells were harvested from confluent cultures and washed three times with 1X PBS buffer at 4 °C. Cell suspension in 1X PBS containing 3×10^6 cells per tube were mixed respectively with 1000, 250 and 50 µg of soluble delipidated His-tagged Mp1p-LBD1 protein on ice. The mixture was immediately sonicated on ice for 20 sec, followed by incubation on ice for 30 min in the presence of 10

µg/ml complete protease inhibitor mixture (Roche Applied Science). Cell pellet was deposited after centrifuging at 10,000×g for 15 min. The supernatant layer was then incubated with 30 µl of Ni-NTA agarose resin (Qiagen) at 4 ºC for 30 min. The resin was washed with twenty column volumes of 1X PBS buffer supplemented with 10 mM imidazole. Lipid-bound His-tagged Mp1p-LBD1 protein was eluted with 200 µl of PBS buffer containing 200 mM imidazole. Bound-lipids in the Mp1p-LBD1 protein were extracted by incubating with organic solvent mixture (DIPE and n-butanol (3:2 v/v)) at 1:1 ratio for 30 min at room temperature. The organic layer was separated by centrifugation (2 min, 13000 rpm) and subjected to untargeted small molecule profiling by ultra-high-performance liquid chromatography-electrospray ionization-quadruple time-of-flight mass spectrometry (UHPLC-ESI-QTOFMS) using lipid profiling method, to analyse lipid species as we have previously described (32, 33). Control pull-down experiments without adding Mp1p-LBD1 to LPS-induced J774 cells were performed under the same procedures. Three biological replicates were performed for each pull-down experiment, and triplicate measurements were made for each pull-down condition.

Untargeted pull-down extract profiling using UHPLC-ESI-QTOFMS

UHPLC-ESI-QTOFMS analysis was performed using M-class UHPLC (Waters, USA) coupled with a Synapt G2-Si HDMS spectrometer (Waters, USA) accompanied with a Masslynx software for QTOF (V 4.1, Waters, USA). Waters Acquity UPLC BEH C18 column (2.1 × 100 mm, 1.7 µm) (Waters, Milford, MA, USA) was applied for the separation of a wide range of lipids with the injection volume of 8 µl. The column and auto-sampler temperature were kept at 45 °C and 10 °C, respectively. Mobile phase A was LC-MS grade water containing 0.1 % acetic acid (v/v) and mobile phase B was acetonitrile. LC separation was achieved at a flow rate of 0.4 ml/min by applying a gradient program as follows: t = 0 min, 0.5 % B; t = 1.5 min, 0.5 % B; t = 8 min, 8 % B; t = 18 min, 35 % B; t = 25 min, 70 % B; t = 34 min, 99.5 % B; t = 36 min, 99.5 % B; t = 38.1 min, 0.5 % B. The total run time was 40 min.

MS Conditions

Mode of Operation	TOF MS^E
Ionization and Capillary voltage	ESI +ve (+3500 V) and –ve (-3500 V)
Cone voltage	20.0 V
Collision energy	20 V & Ramp 30-50 V
Source temperature	120 °C
Desolvation temperature	350 °C
Desolvation gas	500.0 L/Hr (N_2)

Acquisition range	60-1500
Calibrant	Leucine Enkephalin

Data Processing and statistical analysis. The LC-MS data was processed as described by Lau et al (2015) (34). Multi- and uni-variate statistical analyses were carried out to identify specific lipids in extraction samples that are present in significantly higher levels in pull down samples but not in the control samples. Only entries with at least 50 % frequency present in either one of pull-down sample or control groups were included for further statistical analysis to reduce noise. Volcano plots based on $P < 0.01$ combined with fold-change (FC) analysis with $FC > 2$ were applied to highlight molecular features (MFs) with high abundance ratios between 2 groups.

Lipid identification. MFs with significant abundance were selected for MS/MS experiment and analysis. The MS/MS data was processed using Waters MassLynx Analysis software (Version 4.1, Waters, USA) to generate list of potential molecular formula. All putative lipids were identified by using exact molecular weights, nitrogen rule, MS^2 fragment and literature/database search (METLIN, Lipidmaps, etc.). Fatty acid moieties of identified LPCs were determined using fatty acid scanning (FAS) method as described by (12). 5 mM ammonium acetate was spiked into the pull-down lipid extract to yield anion adduct [M + CH3COO-, M + H+58]. FAS analysis was achieved by acquiring precursor ion spectra with selected fragment ions containing 16 to 20 carbon atoms and 0 to 4 double bonds under negative ion mode. Collision energy was ramping from 25 eV to 35 eV.

NMR and isothermal titration calorimetry (ITC) data collection and processing. AA was titrated into a ^{15}N-labeled delipidated sample of Mp1p-LBD1. Two-dimensional ^{1}H-^{15}N heteronuclear single quantum coherence (2D NHSQC) experiments were acquired at 299.1 K on a Bruker Avance 600 MHz NMR spectrometer (^{1}H and ^{15}N frequencies of 600.133 and 60.818 MHz, respectively) equipped with a 5-mm BBI probe with Z-gradient using standard Bruker pulse sequences. Data were acquired and analyzed using Topspin 3.1 (Bruker). Chemical shifts are given on a ppm scale and coupling constants are reported in Hz. All ^{1}H chemical shifts were referenced to trimethylsilylpropanoic acid methyl resonance at 0 ppm. Chemical shifts of ^{15}N were referenced indirectly by gyromagnetic ratio method. Free induction decays were multiplied with an exponential line broadening function of 0.3 Hz before Fourier transformation. The sizes of F2 dimension were 2048 points and that of F1 dimension was 256 points, which were Fourier-transformed into 2048 x 1024 points. Spectral widths were 9014.423 x 2736.807 Hz. Delipidated Mp1p-LBD1 protein samples (100 mM) were loaded into the sample cells and titrated with an AA stock solution of 10 mM by an iTC200 microcalorimeter (Ultrasensitive Calorimetry for the Life Science, MicroCal). The starting temperature was 37℃, and the reference in the reference cell was pure autoclaved

water. The titrations were performed by injecting 20 consecutive 5 ul aliquots of AA stock solution into the ITC cell containing the Mp1p-LBD1 sample. The titration experiment was performed in triplicate. The binding stoichiometry (n), binding affinity (K_d), enthalpy changes (ΔH), and entropy (ΔS) of the protein-ligand interaction were determined by analyzing the resulting ITC data with the software ORIGIN 7 using appropriate binding models.

Accession codes: Mp1p-LBD1 in complex with co-purified PLM was deposited with PDB accession code 5E7X. Mp1p-LBD1 in complex with AA was deposited with PDB accession code 5ECF. Mp1p-LBD1-LBD2 was deposited with PDB accession code 5X3Q.

Acknowledgements

This work was supported by the Natural Science Foundation of China grants (31370739 and 31670753), donation by Mr. Michael Tong and the Providence Foundation in memory of Mr. and Mrs. L.H.M. Lui; Health and Medical Research Fund (commissioned study) of the Food and Health Bureau of Hong Kong Special Administrative Region (HKM-15-M05, HKM-15-M07), Research Grant Council Fund of Hong Kong (GRF777512 and GRF17124717, AoE/P-705/16) and research grant from Shenzhen Innovation Committee of Science and Technology (JCYJ20160608140912962). W.H.L. acknowledges the award of an exchange scholarship that allowed him to spend 12 months with Prof. Samar Hasnain at the University of Liverpool during which time data collection at DIAMOND and SOLEIL were performed. Use of SOLEIL was part funded by the European Community's Seventh Framework Program (FP7/2007-2013) under BioStruct-X (grant agreement number 283570 and proposals number 2370/5437 to S.V.A. and Hasnain). We would like to thank Dr. Y. Zhao's group (The Hong Kong Polytechnic University, Hong Kong) for help with the SLS measurements. We would like to thank technical supports and management from different synchrotrons used in this work: dataset of Mp1p-LBD1-PLM was collected at beamline IO2, DIAMOND, UK; dataset of Mp1p-LBD1-AA was collected at beamline PROXIMA-1, SOLEIL, France; dataset of Mp1p-LBD2-AA was collected at beamline BL13B1, NSRRC, Taiwan, ROC; dataset of Mp1p-LBD1-LBD2 was collected at beamline BL17U, SSRF, China.

Conflict of interest statement: The authors declare no competing financial interests.

Reference

1. Cooper CR, Vanittanakom N. 2008. Insights into the pathogenicity of Penicillium marneffei. Future Microbiology 3:43-55.
2. Ustianowski AP, Sieu TP, Day JN. 2008. Penicillium marneffei infection in HIV. Curr Opin Infect Dis 21:31-6.
3. Wong SS, Siau H, Yuen KY. 1999. Penicilliosis marneffei--West meets East. J Med Microbiol 48:973-5.
4. Vanittanakom N, Cooper CR, Jr., Fisher MC, Sirisanthana T. 2006. Penicillium marneffei infection and recent advances in the epidemiology and molecular biology aspects. Clin Microbiol Rev 19:95-110.
5. Yang E, Wang G, Woo PC, Lau SK, Chow WN, Chong KT, Tse H, Kao RY, Chan CM, Che X, Yuen KY, Cai JJ. 2013. Unraveling the molecular basis of temperature-dependent genetic regulation in Penicillium marneffei. Eukaryot Cell 12:1214-24.
6. Youngchim S, Vanittanakom N, Hamilton AJ. 1999. Analysis of the enzymatic activity of mycelial and yeast phases of Penicillium marneffei. Med Mycol 37:445-50.
7. Cao L, Chan CM, Lee C, Wong SS, Yuen KY. 1998. MP1 encodes an abundant and highly antigenic cell wall mannoprotein in the pathogenic fungus Penicillium marneffei. Infect Immun 66:966-73.
8. Cao L, Chan KM, Chen D, Vanittanakom N, Lee C, Chan CM, Sirisanthana T, Tsang DN, Yuen KY. 1999. Detection of cell wall mannoprotein Mp1p in culture supernatants of Penicillium marneffei and in sera of penicilliosis patients. J Clin Microbiol 37:981-6.
9. Liao S, Tung ET, Zheng W, Chong K, Xu Y, Dai P, Guo Y, Bartlam M, Yuen KY, Rao Z. 2010. Crystal structure of the Mp1p ligand binding domain 2 reveals its function as a fatty acid-binding protein. J Biol Chem 285:9211-20.
10. Woo PCY, Lau SKP, Lau CCY, Tung ETK, Chong KTK, Yang FJ, Zhang HM, Lo RKC, Cai JP, Au-Yeung RKH, Ng WF, Tse H, Wong SSY, Xu SM, Lam WH, Tse MK, Sze KH, Kao RY, Reiner NE, Hao Q, Yuen KY. 2016. Mp1p Is a Virulence Factor in Talaromyces (Penicillium) marneffei. Plos Neglected Tropical Diseases 10.
11. Sze KH, Lam WH, Zhang H, Ke YH, Tse MK, Woo PC, Lau SK, Lau CC, Cai JP, Tung ET, Lo RK, Xu S, Kao RY, Hao Q, Yuen KY. 2017. Talaromyces marneffei Mp1p Is a Virulence Factor that Binds and Sequesters a Key Proinflammatory Lipid to Dampen Host Innate Immune Response. Cell Chem Biol doi:10.1016/j.chembiol.2016.12.014.
12. Ekroos K, Ejsing CS, Bahr U, Karas M, Simons K, Shevchenko A. 2003. Charting molecular composition of phosphatidylcholines by fatty acid scanning and ion trap MS3 fragmentation. J Lipid Res 44:2181-92.
13. Schroeder HW, Jr., Cavacini L. 2010. Structure and function of immunoglobulins. The Journal of allergy and clinical immunology 125:S41-S52.
14. Hammarstrom S, Hamberg M, Samuelsson B, Duell EA, Stawiski M, Voorhees JJ. 1975. INCREASED CONCENTRATIONS OF NONESTERIFIED ARACHIDONIC-ACID, 12L-HYDROXY-5,8,10,14-EICOSATETRAENOIC ACID, PROSTAGLANDIN-E2, AND PROSTAGLANDIN-F2ALPHA IN EPIDERMIS OF PSORIASIS. Proceedings of the National Academy of Sciences of the United States of America 72:5130-5134.
15. Ramanadham S, Gross R, Turk J. 1992. ARACHIDONIC-ACID INDUCES AN INCREASE IN THE CYTOSOLIC CALCIUM-CONCENTRATION IN SINGLE PANCREATIC-ISLET BETA-CELLS. Biochemical and Biophysical Research Communications 184:647-653.
16. Chilton FH, Fonteh AN, Surette ME, Triggiani M, Winkler JD. 1996. Control of arachidonate levels within inflammatory cells. Biochimica Et Biophysica Acta-Lipids and Lipid Metabolism 1299:1-15.
17. Brash AR. 2001. Arachidonic acid as a bioactive molecule. Journal of Clinical Investigation 107:1339-1345.

18. Yuen KY, Chan CM, Chan KM, Woo PCY, Che XY, Leung ASP, Cao L. 2001. Characterization of AFMP1: a novel target for serodiagnosis of aspergillosis. Journal of Clinical Microbiology 39:3830-3837.
19. Chan CM, Woo PCY, Leung ASP, Lau SKP, Che XY, Cao L, Yuen KY. 2002. Detection of antibodies specific to an antigenic cell wall galactomannoprotein for serodiagnosis of Aspergillus fumigatus aspergillosis. Journal of Clinical Microbiology 40:2041-2045.
20. Woo PCY, Chan CM, Leung ASP, Lau SKP, Che XY, Wong SSY, Cao L, Yuen KY. 2002. Detection of cell wall galactomannoprotein Afmp1p in culture supernatants ofAspergillus fumigatus and in sera of aspergillosis patients. Journal of Clinical Microbiology 40:4382-4387.
21. Woo PCY, Chong KTK, Leung ASP, Wong SSY, Lau SKP, Yuen KY. 2003. AFLMP1 encodes an antigenic cell wall protein in Aspergillus flavus. Journal of Clinical Microbiology 41:845-850.
22. Chong KTK, Woo PCY, Lau SKP, Huang Y, Yuen KY. 2004. AFMP2 encodes a novel immunogenic protein of the antigenic mannoprotein superfamily in Aspergillus fumigatus. Journal of Clinical Microbiology 42:2287-2291.
23. Woo PCY, Chong KTK, Lau CCY, Wong SSY, Lau SKP, Yuen KY. 2006. A novel approach for screening immunogenic proteins in Penicillium marneffei using the Delta AFMP1 Delta AFMP2 deletion mutant of Aspergillus fumigatus. Fems Microbiology Letters 262:138-147.
24. Wang ZY, Cai JP, Qiu LW, Hao W, Pan YX, Tung ETK, Lau CCY, Woo PCY, Lau SKP, Yuen KY, Che XY. 2012. Development of monoclonal antibody-based galactomannoprotein antigen-capture ELISAs to detect Aspergillus fumigatus infection in the invasive aspergillosis rabbit models. European Journal of Clinical Microbiology & Infectious Diseases 31:2943-2950.
25. Woo PCY, Lau SKP, Lau CCY, Tung ETK, Au-Yeung RKH, Cai JP, Chong KTK, Sze KH, Kao RY, Hao Q, Yuen KY. 2018. Mp1p homologues as virulence factors in Aspergillus fumigatus. Medical Mycology 56:350-360.
26. Kabsch W. 2010. XDS. Acta Crystallogr D Biol Crystallogr 66:125-32.
27. Otwinowski Z, Minor W. 1997. Processing of X-ray diffraction data collected in oscillation mode. Macromolecular Crystallography, Pt A 276:307-326.
28. McCoy AJ, Grosse-Kunstleve RW, Adams PD, Winn MD, Storoni LC, Read RJ. 2007. Phaser crystallographic software. J Appl Crystallogr 40:658-674.
29. Emsley P, Lohkamp B, Scott WG, Cowtan K. 2010. Features and development of Coot. Acta Crystallographica Section D-Biological Crystallography 66:486-501.
30. Murshudov GN, Vagin AA, Dodson EJ. 1997. Refinement of macromolecular structures by the maximum-likelihood method. Acta Crystallogr D Biol Crystallogr 53:240-55.
31. Chen VB, Arendall WB, 3rd, Headd JJ, Keedy DA, Immormino RM, Kapral GJ, Murray LW, Richardson JS, Richardson DC. 2010. MolProbity: all-atom structure validation for macromolecular crystallography. Acta Crystallogr D Biol Crystallogr 66:12-21.
32. To KK, Lee K-C, Wong SS, Sze K-H, Ke Y-H, Lui Y-M, Tang BS, Li IW, Lau SK, Hung IF. 2016. Lipid metabolites as potential diagnostic and prognostic biomarkers for acute community acquired pneumonia. Diagnostic Microbiology and Infectious Disease.
33. To KKW, Lee KC, Wong SSY, Lo KC, Lui YM, Jahan AS, Wu AL, Ke YH, Law CY, Sze KH, Lau SKP, Woo PCY, Lam CW, Yuen KY. 2015. Lipid mediators of inflammation as novel plasma biomarkers to identify patients with bacteremia. Journal of Infection 70:433-444.
34. Lau SK, Lam CW, Curreem SO, Lee KC, Lau CC, Chow WN, Ngan AH, To KK, Chan JF, Hung IF, Yam WC, Yuen KY, Woo PC. 2015. Identification of specific metabolites in culture supernatant of Mycobacterium tuberculosis using metabolomics: exploration of potential biomarkers. Emerg Microbes Infect 4:e6.
35. Dugan LL, Kim-Han JS. 2004. Astrocyte mitochondria in in vitro models of ischemia. Journal of Bioenergetics and Biomembranes 36:317-321.

752

753 **Table 1.** Data collection and refinement statistics of X-ray structures (molecular
754 replacement)

	Mp1p-LBD1-PLM	Mp1p-LBD1-AA	Mp1p-LBD1-LBD2
Data collection			
Space group	$P4_3$	$P2_1$	$P4_12_12$
Cell dimensions			
a, *b*, *c* (Å)	52.58,52.58,57.69	65.68,104.27,108.10	146.36,146.39,148.61
α,β,γ (º)	90.00, 90.00, 90.00	90.00, 97.44, 90.00	90.00, 90.00, 90.00
Resolution (Å)	38.86-1.8 (1.85-1.80)*	107.19-2.60 (2.69-2.60)	50.00-4.20 (4.35-4.20)
R_{sym} or R_{merge}	0.027 (0.583)	0.074 (0.390)	0.153 (0.000)
I / σI	22.7 (1.8)	12.6 (2.16)	9.520 (1.74)
Completeness (%)	99.1 (95.6)	94.4 (69.7)	99.7 (100.0)
Redundancy	3.7 (3.6)	3.6 (2.8)	6.2 (6.3)
Refinement			
Resolution (Å)	45.00-1.45 (1.85-1.80)	107.19-2.60 (2.69-2.60)	50-4.20 (4.35-4.20)
No. reflections	14575	44571	12286
R_{work} / R_{free}	0.179/0.221	0.256/0.290	0.2943/0.3496
No. atoms			
Protein	1151	10929	3217
Ligands	18	88	N/A
Water	53	19	N/A
B-factors			
Protein	36.23	38.51	135.31
Ligands	44.55	32.20	N/A
Water	40.35	36.60	N/A
R.M.S. deviations [#]			
Bond lengths (Å)	0.0071	0.0169	0.0106
Bond angles (º)	1.1528	1.0730	1.2520
MolProbity validation			

MolProbity scores (percentile)	0.84 (100th)	1.98 (97th)	1.96 (100th)
Clashscores (percentile)	1.24 (100th)	12.79 (93th)	12.87 (97th)
Ramachandran favored/outliers(%)	99.35/0	98.48/0.07	95.15/0.49

*Values in parentheses are for highest resolution shells.

[#] R.M.S deviations mean root-mean-square deviations.

Table 2. Cellular level of arachidonic acid (AA) in J774 cells in non-infected and infected with Mp1p knockout and wild-type strains of *T. marneffei* conditions.

	Non-infected	Mp1p knockout *T. marneffei*	wild-type *T. marneffei*
MS extract sample [AA] (nM)[a]	583±36	550±30	470±20
AA (pmole/1x10^6 cells)[b]	35.0±2.2	33.0±1.8	28.2±0.9
Cellular [AA] (μM) [c]	3.50	3.30	2.82

[a] AA concentration in 180 μl extraction buffer from cell lysate containing 3×10^6 cells

[b] Amount of AA in sample normalized to 1×10^6 cells

[c] Assuming a cellular volume of ~ 10 μl per 1x10^6 J774 cells

766 **Table 3.** *In vitro* pull-down experiments with various amount of Mp1p-LBD1 against cell
767 lysates of J774 macrophage cells:

768 **(A)** Profile list of identified lipids from the organic layer extracted under different amount of
769 Mp1p-LBD1 bait protein.

Low Mp1p-LBD1 (50mg)	**Medium Mp1p-LBD1 (250mg)**	**High Mp1p-LBD1 (1000mg)**
Arachidonic Acid	Arachidonic Acid	Arachidonic Acid
Oleic Acid	Oleic Acid	Oleic Acid
-	Palmitic Acid	Palmitic Acid
-	LPC1, 482.3612	LPC1, 482.3612
-	LPC2, 496.3413	LPC2, 496.3413
-	-	LPC3, 522.3559
-	-	LPC4, 524.2736

770 *LPC= lysophosphatidylcholine

771 **(B)** The identity of each LPC was not characterized. All LPC ions give rise to the same
772 characteristic fragment ion (m/z = 184.0735) in high energy mode (Collision energy CE
773 =30-50eV).

PIS (M+H, 184.1)		**FAS[b]**		**Remarks**
Precursor Ion	Brutto Composition[a]	Precursor Ion	Fatty Acid Moieties	
496.4	16:0	554.5	16:0	Palmitoyl-LPC
482.4	16:0	540.5	16:0	LPC(O-16:0), Lyso-PAFC16
522.4	18:1	580.5	18:1	Oleoyl-LPC
524.4	18:0	602.5	18:0	LPC(18:0)

774 [a] Number of carbon: Number of double bond

775 [b] Fatty acid scanning (35) = 255.2 (16:0), 281.2 (18:1), 283.2 (18:0)

776 [c] Fatty acid moieties of identified LPCs were determined using fatty acid scanning (FAS)
777 method as described by Ekroos et al (2003) (12)

778 *LPC= lysophosphatidylcholine; PAF=platelet-activating factor

779

Figure Captions

Figure 1. Crystallographic structure of Mp1p-LBD1 in complex with co-purified PLM at 1.80Å resolution. (A) Overall monomeric structure of Mp1p-LBD1 complexed with PLM (shown in cyan spheres). The length of this domain was about 47Å. (B) Alignments of this monomeric Mp1p-LBD1 structure (green) with two domain-swapped, open Mp1p-LBD2 complexed with palmitic acid (PDB 3L1N, magenta and blue) (left, 762 main chain atoms with RMS = 0.668Å) and monomeric Mp1p-LBD2 complexed with arachidonic acid (PDB 5CSD, red) (right, 811 main chain atoms with RMS = 0.538Å). The helix 3 of Mp1p-LBD1 resembled the same helix in 5CSD, but not 3L1N (regions highlighted in orange boxes), in which helix 3 turns and breaks the continuation at conserved glycine residue (indicated by arrows in corresponding colours). (C) 2mFo-DFc map (green, contour level: 1.0σ) of PLM in refined model. (D) The amino acid residues involved in interaction between co-purified PLM and Mp1p-LBD1.

Figure 2. Superposition of different Mp1p-LBD structures with different ligands positions revealed a possible reason of domain-swapping in Mp1p-LBD2 in crystal structures. (A) Alignment of helices 3 from Mp1p-LBD1 complexed with PLM (orange) and Mp1p-LBD2 complexed with AA (5CSD, cyan) near the "hinge" regions. (B) Alignment of H3 helices from Mp1p-LBD1 complexed with PLM (orange) and LBD2 complexed with PLM (3L1N, green and purple for the helix 3 from another Mp1p-LBD2 monomer) near the "hinge" regions. The PLM in Mp1p-LBD1 and AA in Mp1p-LBD2 locate near the hinge points of both Mp1p-LBDs, providing additional hydrophobic interactions around this region which may stabilize the closed configuration during crystallization. PLM in Mp1p-LBD2, however, locates on the other side of the binding cavity, leading to the absence of the hydrophobic interaction and may lead to domain-swapped open structure as observed in 3L1N.

Figure 3. Mp1p-LBD1 complexed with 1 or 2 AAs. (A) Overall closed monomeric structures of Mp1p-LBD1 complexed with 1 AA molecule (Left) and 2 AA molecules (Right). Bound AAs are shown in cyan spheres at the middle of the five-helical bundles. (B) 2mFo-DFc maps (green, contour level: 1.0σ) of AA in refined models. Top: singly-bound AA. Bottom: Two AAs in 2-AAs bound form. (C) Detailed interaction between AA and Mp1p-LBD1. Left panel: Singly-bound AA in Mp1p-LBD1-AA form. Middle panel: AA_a in Mp1p-LBD1-2AA form. Ser165 also provides hydrogen bond. Right panel: AA_b in Mp1p-LBD1-2AA on the other side of the cavity.

Figure 4. Asn105 in Mp1p-LBD1 provides additional hydrogen bond to bind AA, leading to shifted AA positions compared to AAs in Mp1p-LBD2. (A) Superposition of Mp1p-LBD1-1AA (pink) and Mp1p-LBD1-2AAs (green). AA_a in Mp1p-LBD1-2AA superimposes the singly-bound AA. Asn105 is involved to form hydrogen bond with bound AA in both forms. (B) Superposition of Mp1p-LBD1-1AA (pink) and Mp1p-LBD2-1AAs (orange). It is clear that the interlude of Asn105 preferentially forms hydrogen bond with singly-bound AA in Mp1p-LBD1, while the singly-bound AA in Mp1p-LBD2 penetrates deeper into the cavity and form hydrogen bond with the conserved glutamine residue (Gln298 in Mp1p-LBD2). (C) Superposition of Mp1p-LBD1-2AA (green) and Mp1p-LBD2-2AAs (Blue). The conformation of the 2 bound AAs are largely conserved in both Mp1p-LBDs, but the positions of the head groups differ due to additionally available hydrogen bond partner from Asn105 in Mp1p-LBD1.

Figure 5. Crystal structure of Mp1p-LBD1-LBD2 at 4.20Å resolution. (A) Pseudo-dimeric structure of Mp1p-LBD1-LBD2. Two monomers are colored in green and yellow, respectively. (B) Structure at Mp1p-LBD2 hinge point Gly259 of helix 3 (in full, shown in red) causing the open conformation of Mp1p-LBD2. This part is thus the same as the single domain Mp1p-LBD2-PLM structure (PDB 3L1N). (C) The two modelled linkers (shown in red) built between two pairs of Mp1p-LBD1 and Mp1p-LBD2.

Figure 6. *In vitro* pull-down experiments with various amount of Mp1p-LBD1 against cell lysates of J774 macrophage cells. (A) Profile list of identified lipids from the organic layer extracted under different amount of Mp1p-LBD1 bait protein. (B) The identity of each LPC was not characterized. All LPC ions give rise to the same characteristic fragment ion (m/z = 184.0735) in high energy mode (Collison energy CE =30-50eV). Fatty acid moieties of identified LPCs were determined using fatty acid scanning (FAS) method as described by Ekroos et al (2003) (12).

Figure 7. NMR titration experiments of 15N-Mp1p-LBD1 with AA.1H-15N HSQC titration spectra of 15N-Mp1p-LBD1 in the absence (blue) and presence (red) of AA. Mp1p-LBD1 was titrated against AA at pH 8.0. Most peaks displayed slow exchange (peak weakening) while some show fast exchange (peak shifting)

Figure 8. Isothermal Titration Calorimetry (ITC) of AA binding to Mp1p-LBD1. (Top panels) Raw heats of binding obtained by ITC when AA was mixed with Mp1p-LBD1. (Bottom panels) Table of thermodynamic parameters obtained by fitting the ITC data to a two-site binding model (Kd = dissociation constant, ΔH = change in enthalpy, $-T\Delta S$ = change in entropy, N = number of binding sites, subscript 1 and 2 refer to the 1st and 2nd binding step for data fit to a two-site model.

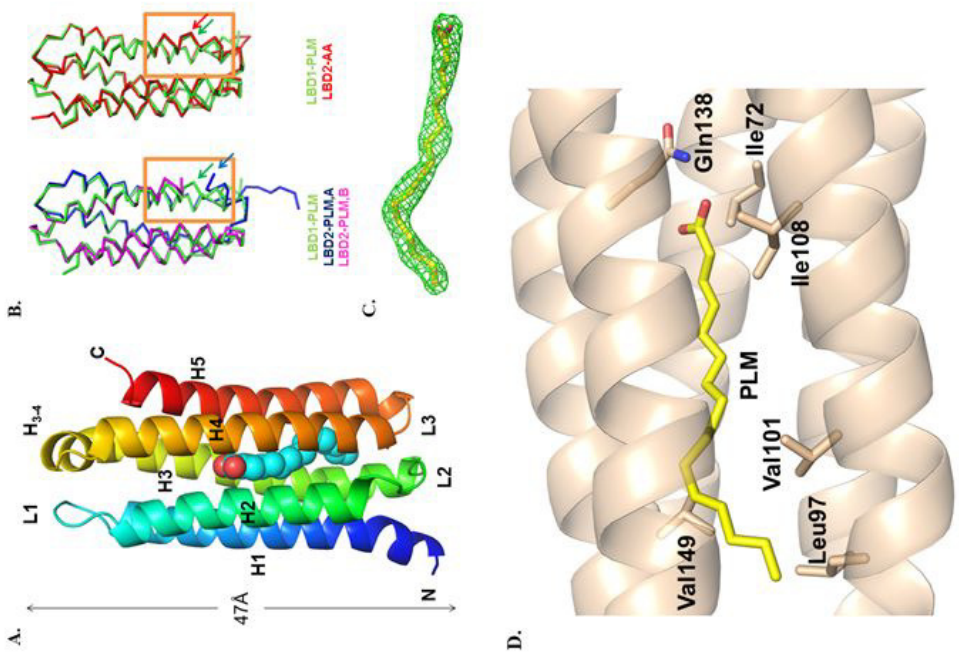

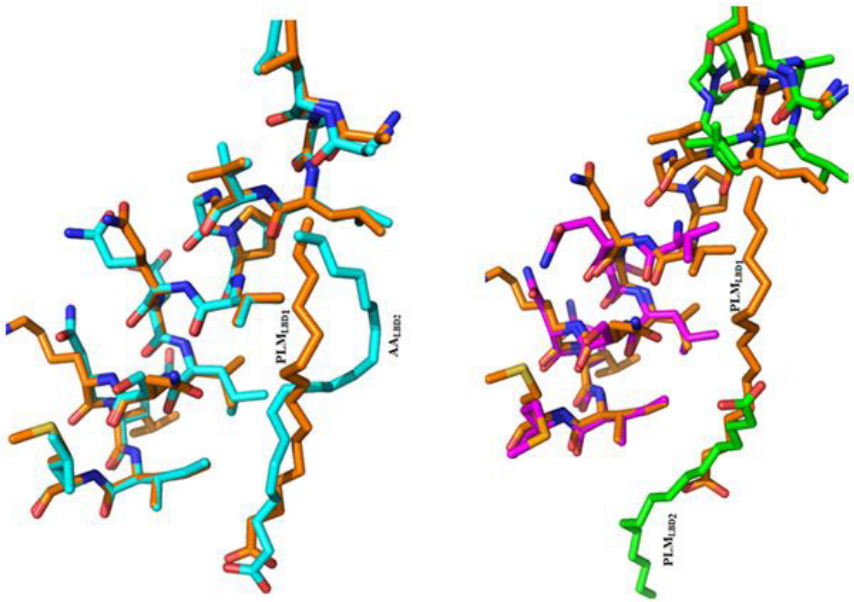

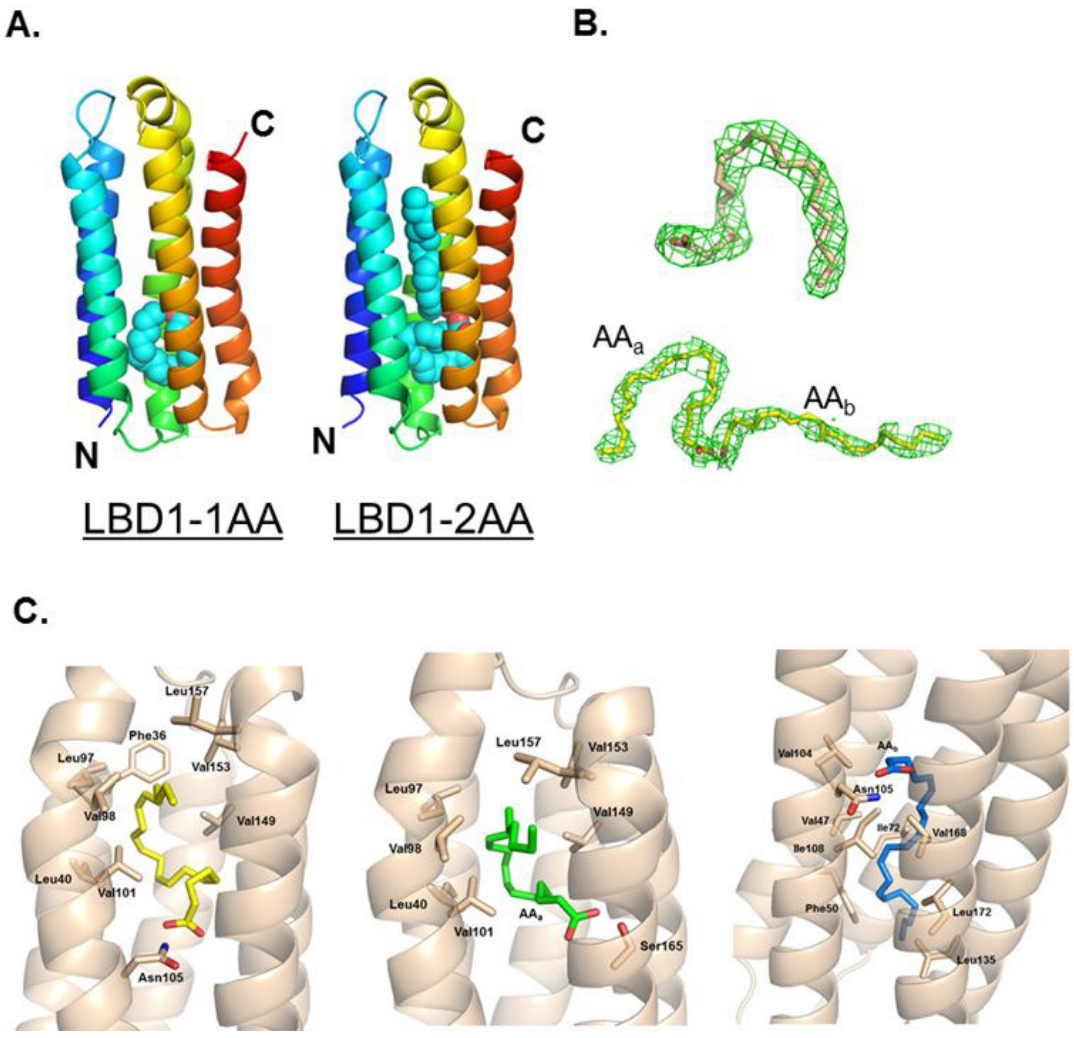

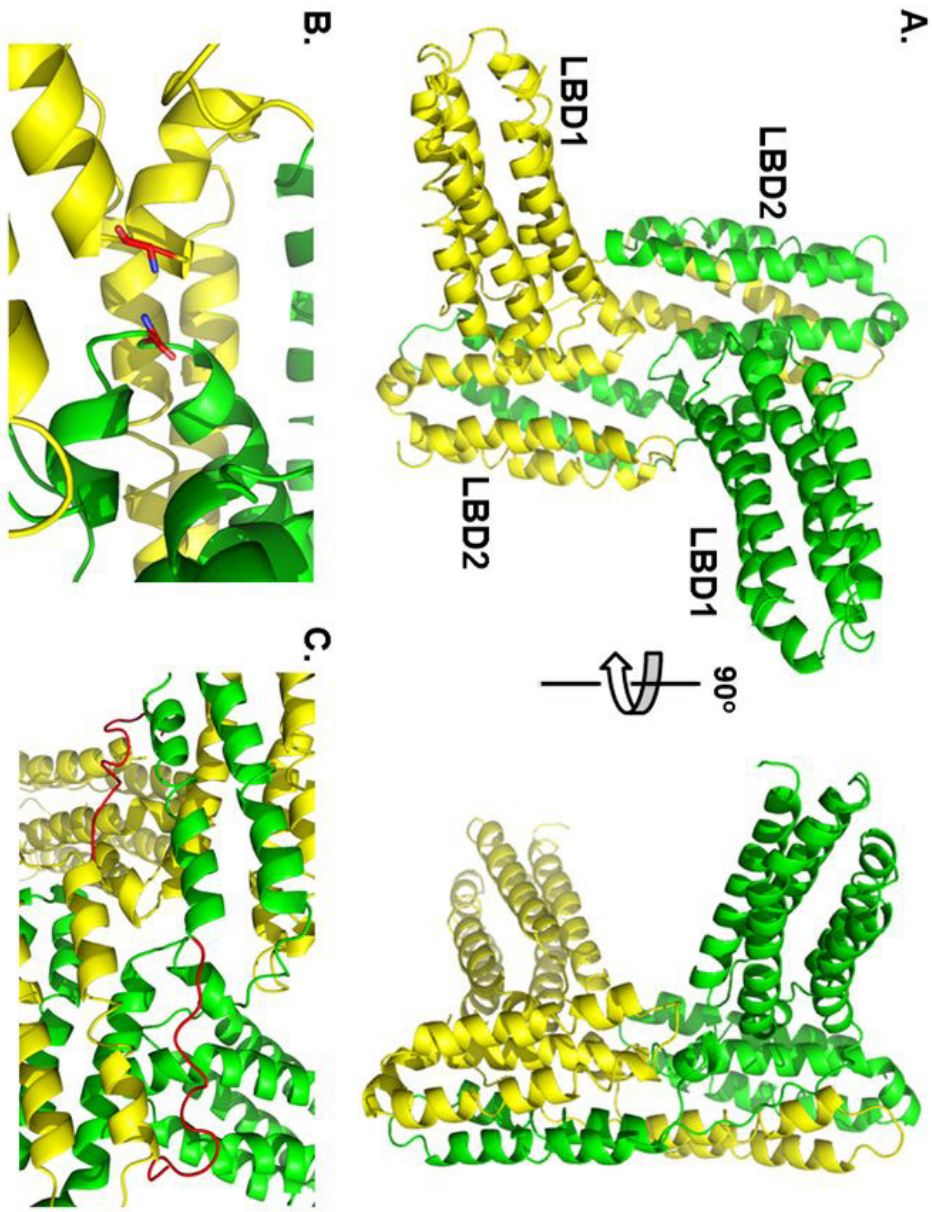

(A)

Low LBD1 50 ug	Medium LBD1 250 ug	High LBD1 1000 ug
Arachidonic Acid	Arachidonic Acid	Arachidonic Acid
Oleic Acid	Oleic Acid	Oleic Acid
	Palmitic Acid	Palmitic Acid
	LPC1,482.3612	LPC1,482.3612
	LPC2,496.3413	LPC2,496.3413
		LPC3,522.3559
		LPC4,524.2736

(B)

PIS (M+H,184.1)		FAS[b]		
Precursor Ion	Brutto Composition[a]	Precursor Ion	Fatty Acid Moieties	Remarks
496.4	16:0	554.5	16:0	Palmitoyl-LPC
482.4	16:0	540.5	16:0	LPC(O-16:0),Lyso-PAF-C16
522.4	18:1	580.5	18:1	Oleoyl-LPC
524.4	18:0	602.5	18:0	LPC(18:0)

[a] Number of carbon : Number of double bond

[b] Fatty acid scaning [M-H]=255.2(16:0), 281.2(18:1), 283.2(18:0)

(C)

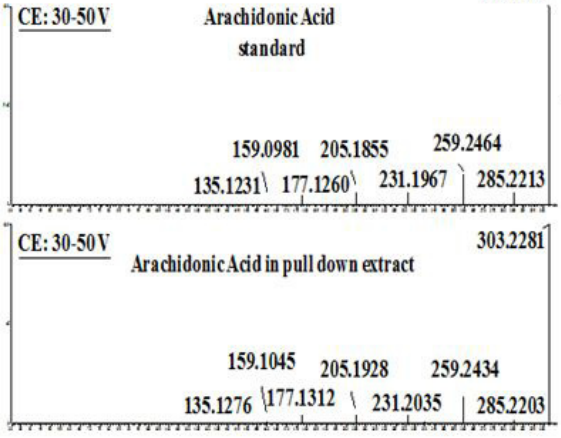

(D)

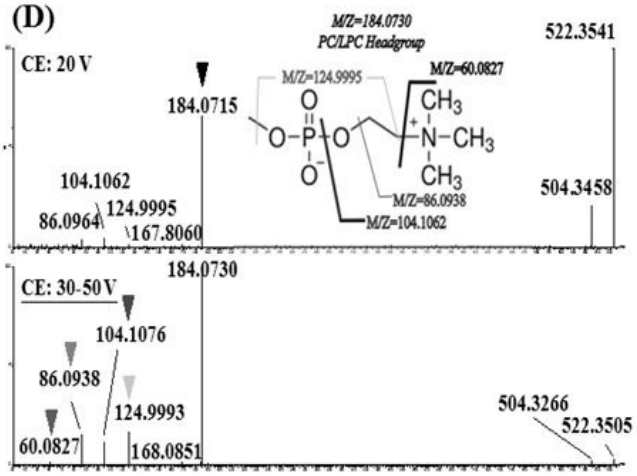

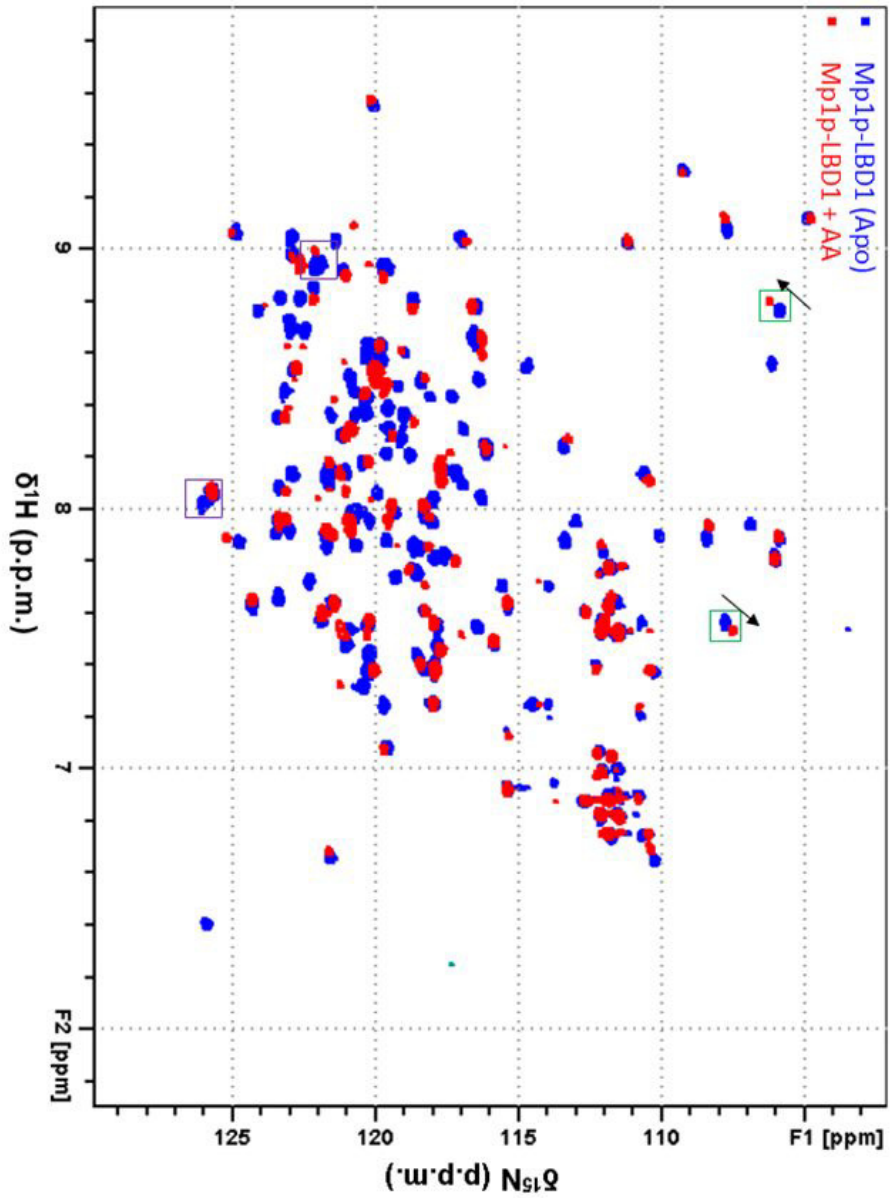

A

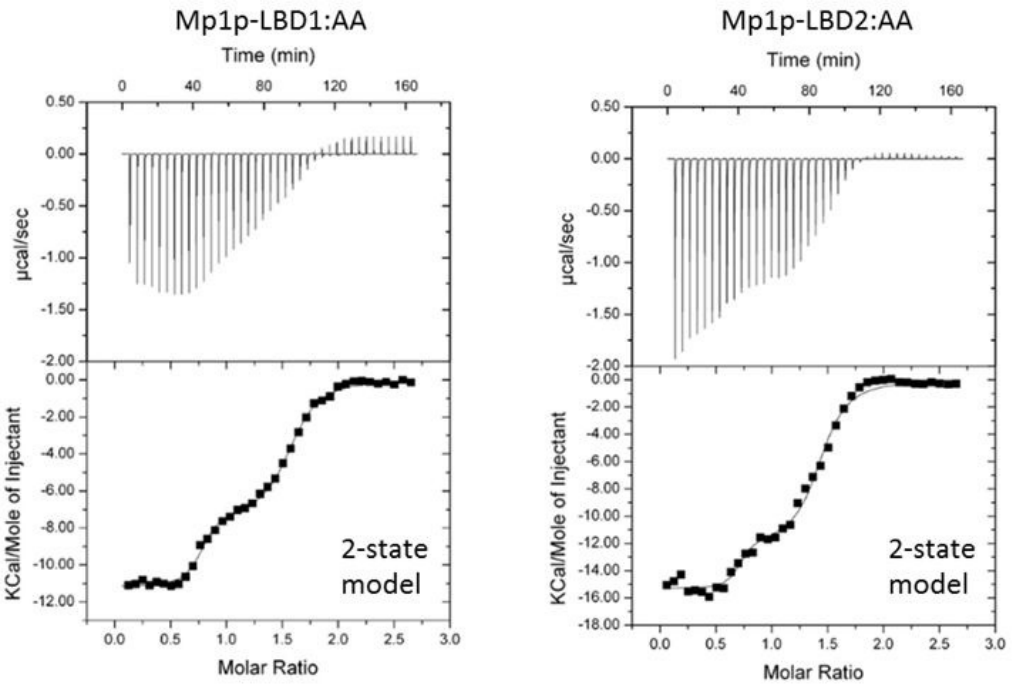

B

Analyte	N_1	K_{d1}	ΔH_1 (Kcal/mol)	$-T\Delta S_1$ (Kcal/mol)	N_2	K_{d2}	ΔH_2 (Kcal/mol)	$-T\Delta S_2$ (Kcal/mol)
Mp1p-LBD2	0.67	13 nM	-14.2	3.4	0.81	2.3 µM	-11.0	2.3
Mp1p-LBD1	0.75	24 nM	-11.2	0.8	0.81	2.3 µM	-7.4	-0.3